

**NEW METHODOLOGIES FOR ASSESSING CAVITATION LOAD
AND RESISTANCE OF STRUCTURAL MATERIALS
AND PROTECTIVE COATINGS IN NUCLEAR POWER INDUSTRY.
PART I. MONOFRACTIONAL APPROACH**

Vladimir Safonov¹, Janusz Steller², Ilya Klimenko¹, Aleksandr Kuprin¹
¹National Science Center “Kharkov Institute of Physics and Technology”,

Kharkiv, Ukraine;

*²Szewalski Institute of Fluid-Flow Machinery of the Polish Academy of Sciences,
Gdansk, Poland*

E-mail: steller@imp.gda.pl, safonov600@gmail.com

The paper presents a new method for assessing the cavitation load and durability of structural materials and protective coatings. To determine the cavitation load on a rotating disk or other test rig, a new method for extracting erosion loads based on tests of reference materials on a reference cavitation rig is proposed. Direct measurements of the cavitation load in a cavitation tunnel with a slot cavitator, performed using piezoelectric sensors, made it possible to obtain information on the spatial distribution of the impact load. As an analytical function for modeling cumulative erosion curves in the monofractional approach, the logarithmic formula of L. Sitnik is used, assuming that cavitation erosion is a stochastic process described using fatigue theory. Armco iron is chosen as a reference material, in view of the weak dependence of its erosion rate on cavitation qualitative features. Therefore the local load value could have been extracted from the eroded surface profile of the Armco iron sample. Using the example of TiN coating analysis on stainless steel and VT3-1 titanium alloy, the time dependencies and threshold characteristics of their resistance were determined depending on the parameter of the density of the supplied energy.

1. INTRODUCTION

Although cavitation was anticipated by L. Euler in 1756 [1], it was not until the beginning of the last century that cavitation was identified as one of the major limitations in the further development of high-speed hydroturbine machines and other equipment. The study of cavitation dates back to the seminal work of Rayleigh in 1917 [2]. Studying the growth and subsequent collapse of bubbles in water, Rayleigh proposed a simple model that estimates the internal pressure in a collapsing spherical cavity. Since then, the intense collapse of bubbles that form near solid surfaces has been widely studied and continues to this day. The significance of the problem became even better understood when it came to the development of advanced technologies in the aerospace and nuclear industries in the middle of the last century. It should be noted that the boom of the nuclear industry in the 1960s and 1970s was accompanied by a number of studies devoted to cavitation not only in water, but also in sodium, mercury and other liquid metals used as coolants for nuclear reactors. Maintaining the highest safety standards for nuclear cooling systems is generally considered extremely important, since most nuclear incidents to date have been associated with cooling system failures, as well as in cases requiring repair work related to cavitation-droplet erosion of turbine blade material [3]. Impacts and instantaneous pressure peaks due to the collapse of steam clouds lead to dynamic loads on the surfaces of materials, which can lead to damage to the material when a certain threshold load level is exceeded. Therefore, it is usually necessary to

avoid cavitation. If cavitation cannot be completely avoided, it is important that this phenomenon does not have a detrimental effect on streamlined surfaces. The stated objective can be achieved by selecting cavitation-resistant structural materials or by applying highly resistant protective coatings. In both cases, a reliable assessment of the resistance of the surface layer to the cavitation load expected in the flow system is of primary importance.

Hardening of surface layers and application of hardening and protective coatings are widely used in modern materials science. This allows for a significant increase in the surface strength, heat resistance, corrosion resistance and, as a result, the service life of structural and tool materials. However, this may reduce the ductility of the material and, as a rule, its fatigue strength, which is most important for protection against cavitation erosion.

Cavitation erosion is a complex phenomenon that includes not only the hydrodynamic factors of the liquid, but also the properties of the eroded material and coating, i.e. adhesion, microstructure, hardness, Young's modulus. In order to predict the service life of turbomachines, it is necessary to accurately measure the cavitation intensity (CI). From an industrial point of view, concerning both the design and maintenance of machines, assessing the erosive capacity of cavitating flows and predicting material damage remain a serious problem for machine manufacturers and users.

In the simplest approach, the cavitation load can be characterized by the cavitation intensity factor, defined as the energy flux density delivered to the surface by

cavitation pressure pulses. The factor is usually calculated using amplitude histograms of the resulting electrical pulses delivered by piezoelectric transducers. In the case of some relatively soft materials (armco iron, lead or zinc), the energy absorption efficiency depends weakly on the pulse amplitude and the volume loss curves plotted against the delivered energy, as determined by the procedure described above. Such materials can be used to estimate the net energy flux delivered by cavitation pulses to a solid surface, using the erosion curves given above as calibration curves.

Modeling of cavitation erosion has made significant progress in recent years, due to the increase in computing power and advanced modeling methods such as computational fluid dynamics (CFD) and fluid-structure interaction (FSI), structural models, etc. [4, 5]. As calculations show, damage to the material due to cavitation phenomena is mainly associated with the energy of the pressure wave emitted by the vapor structures during collapse [6]. The power density of the pressure wave characterizes the aggressiveness of cavitation and is related to the hydrodynamic conditions of the flow.

Numerical calculations together with the analysis of pits on the surface of samples exposed to cavitating flows allow us to estimate the power density of the pressure wave, which characterizes the aggressiveness of the flow. The results showed that the assessment of the power density of the pressure wave is a useful tool for predicting cavitation erosion, assessing the aggressiveness of the cavitation flow and the effect on erosive damage to the material.

In this context, the present work is aimed at an experimental analysis of the amount of energy delivered to the surface during bubble collapse and the erosive effect on the solid surface of the sample.

1.1. FATIGUE STRENGTH AND CAVITATION RESISTANCE

Fatigue is one of the most difficult and insidious problems in mechanical engineering that must be solved. Experience has shown that most structural failures are due to fatigue: the percentage of such failures of mechanical components is about 90%.

Fatigue phenomena are also considered to be the main mechanism of erosion processes, including cavitation erosion processes. An expression of this state of affairs is the classical course of the erosion curve, covering the incubation period during which surface deformations, microcracks and numerous structural deformations – and even phase transformations – occur under the surface layer without noticeable loss of mass. As early as 1955, in the pioneering work of Plesset, the effects of cavitation on polycrystalline samples, as well as on a zinc single crystal, were studied [7]. The metallographic and X-ray structural studies showed that plastic deformation occurs in the samples, damage occurs as a result of cold working, which leads to fatigue and destruction. The mechanism of low-cycle fatigue is mentioned in the model of A. Karimi [8], proposed in the late 1980s and particularly popular in France [9]. In turn, the relationships between fatigue strength determined on the basis of laboratory tests with

random amplitude of the loading cycle and the results of material tests in the Lichtarowicz chamber were analyzed in the 1990s by a team from the Opole University of Technology [10].

Although the impact caused by the collapse of the cavitation bubble causes serious damage to hydraulic machines, it can be used for mechanical surface treatment of metallic materials in the same way as shot peening. Hardening using cavitation action is called cavitation hardening.

An example of load control is the Framatome ultra-high pressure cavitation hardening process, which provides an innovative solution for surface treatment of light water reactors, preventing stress corrosion cracking (SCC) and mitigating ageing. This concerns the key components of the primary circuit system – the reactor head nozzle penetrations (RHNP), the instrument penetrations (IPP) and the primary circuit vessel nozzles [11].

During cavitation hardening, bubbles are constantly formed and destroyed, which leads to high impact loads on the treated surface. At the initial stage of cavitation hardening, the most obvious change is plastic deformation instead of mass loss on the sample surface, which is favorable for the mechanical properties of the surface. In [12], the results of a comparative plane bend fatigue test of stainless steel after processing by different methods are presented. It was concluded that the fatigue strength at $N = 10^7$ with cavitation hardening was the highest, followed by shot peening, immersion laser hardening and, finally, water jet hardening.

However, as the cavitation exposure time increases, erosion and damage occurs on the metal surface due to an increase in the number of failure events. In this regard, the exposure time and the load value are key parameters for the surface properties of the sample during processing.

1.2. PREDICTION OF CAVITATION EROSION

Predicting cavitation erosion under full-scale operating conditions is difficult and relies on laboratory testing using accelerated methods such as:

- ASTM G32-17, Standard Test Method for Cavitation Erosion Using a Vibratory Apparatus. In this method, cavitation is induced by vibrating a immersed specimen at a high frequency (20 kHz);
- ASTM G134-95, Standard Test Method for Erosion of Solids. cavitating liquid jet.

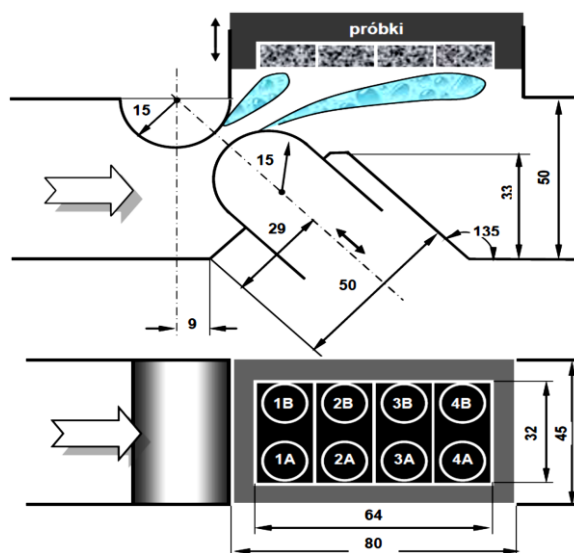
This test method is an alternative to Test Method G32. A immersed cavitating jet exiting a nozzle impacts a test specimen in its path, causing cavities in the specimen to collapse, causing erosion. In this method, cavitation is induced in a flow system designed so that both the jet velocity and the outlet pressure causing the bubbles to collapse can be varied independently.

Laboratory testing devices are widely used to characterize the resistance of various materials to cavitation erosion. As an example, we mention the work of Hattori et al. [13–15], who created a database of 143 materials, including various types of metal alloys, as well as plastics and ceramics. Erosion resistance, defined as the inverse erosion rate (in $\mu\text{m/h}$), was measured under various operating conditions using

1.3. PROBLEMS OF CAVITATION EROSION TESTING

The purpose of this 1st part of this article is to share the experience gained by the authors in developing a methodology for assessing cavitation load and comparing this load with cumulative erosion curves. This experience will be largely used in the next part.

Due to the design features of the rotating disk stand, direct measurement of the cavitation load by sensors is impossible. To determine the equivalent loads on the rotating disk station, erosion tests were carried out in a pipe with a slot cavitation exciter in the IMP PAN laboratory under motion modes selected on the basis of exploratory tests, including visual observations, acoustic measurements (including acoustic emission) and exploratory tests on mass loss on samples [17]. The main element of the pipe is the test chamber (Fig. 1), in which cavitation occurs as a result of a decrease in pressure in an adjustable gap between two semi-cylindrical thresholds. Cavitation clouds breaking away from the surface of the thresholds interact directly with the washed surface of the insert located in the upper wall of the chamber. The position of the insert and the lower obstacle can be adjusted using spacers and a screw mechanism, respectively. As a result, one or another cavitation load can be set on the samples based on the mutual position and flow parameters.



Load measurements were carried out using S113B23 sensors from PCB Piezotronics, working with 480E09 amplifiers from the same company. The signals from the amplifiers were transmitted via a BNC-2110 connector from National Instruments to a NI 6115 data acquisition card from the same company, installed in the

PCI slot of the 32-bit expansion of the external data bus of the laptop. Data recording was carried out under the control of an application created in the DASYLab environment (also National Instrument). The sampling frequency was 1 MHz, the recording time of one signal was 9...10 s.

Cavitation testing of samples was carried out using the rotating disk rig (Fig. 2) in the laboratory of the IFFM Polish Academy of Sciences. The rig is a typical facility used to determine cavitation resistance of structural materials applied in hydraulic machinery and equipment. The achieved cavitation intensity significantly, by two orders of magnitude, exceeds that found in hydraulic machines.

The working disk with a diameter of 310 mm has sockets for eight samples with a diameter of 30 mm, which are installed flush with the disk surface. Cavitation is created by cylindrical bolts (cavitators Φ 12 mm, located on the disk surface along a circle with a diameter of 270 mm in front of each sample. The disk is rotated by an electric motor with a power of 45 kW at a speed of 2950 rpm. Fixed damping blades are installed on the upper cover and under the disk. The parameters of the setup are selected so that the zone of maximum erosion falls on the center of the samples. The load is distributed unevenly over the sample. The load intensity varies over the surface from zero to the maximum value. Water at a temperature of 20 °C was used as the working medium. The average manometric pressure was maintained at a level of 150 kPa.



Fig. 2. Rotating disk test chamber with eight samples

The tests were carried out on four types of samples: armco iron, titanium grade VT3-1 (Ti-6Al-2Mo-1Cr) without coating and with TiN coating, as well as stainless steel 08Cr18Ni10T with TiN coating. The erosion profiles of the samples were studied on a 3D X-ray tomograph (Phoenix v/tome/x m, GE Inspection Technologies GmbH, Germany).

The TiN coatings were deposited by the Arc PVD method using a Bulat-type installation on samples made of titanium alloy (further-Ti) and stainless steel (SS). The deposition parameters were as follows: the distance from the cathode was 200 mm, the vacuum arc discharge current was 135 A, and a negative potential of 200 V was applied to the samples. The initial pressure in the vacuum chamber was $8 \cdot 10^{-4}$ Pa. The nitrogen pressure during the application of TiN coatings was

0.5 Pa. The thickness of the applied coatings ranged from 15 to 18 μ m.

3. RESULTS AND DISCUSSION

3.1. MEASUREMENT OF CAVITATION LOAD

The measurements of the cavitation load on Armco iron samples were carried out in modes selected in advance on the basis of reconnaissance tests [17]. The results of these measurements are shown in Fig. 3. A full description of the study is given in [3]. The results are shown for one of the modes, the tunnel operated at inlet and outlet pressures of $p_1 = 1250$ kPa and $p_2 = 145$ kPa, respectively, and the width of the cavitator gap was 5 mm. The loaded surface was let into the upper wall by 12 mm.

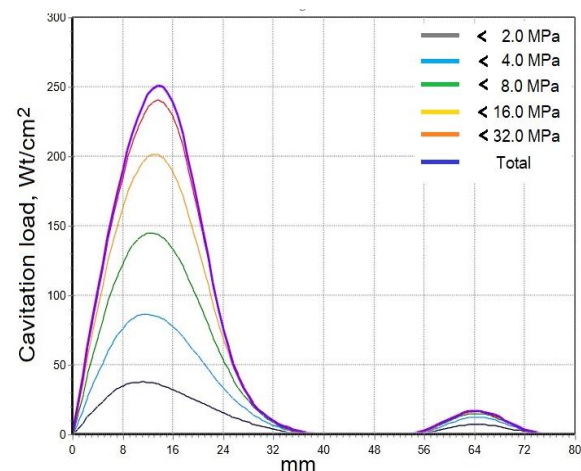


Fig. 3. Distribution of the cavitation load parameter ME along the test insert in the IMP PAN cavitation tunnel

Fig. 4 shows the dependence of the erosion value of Armco iron samples on the test time for three different modes. The results show a significant dependence of the erosion rate on the test conditions associated with different aggressiveness of cavitation.

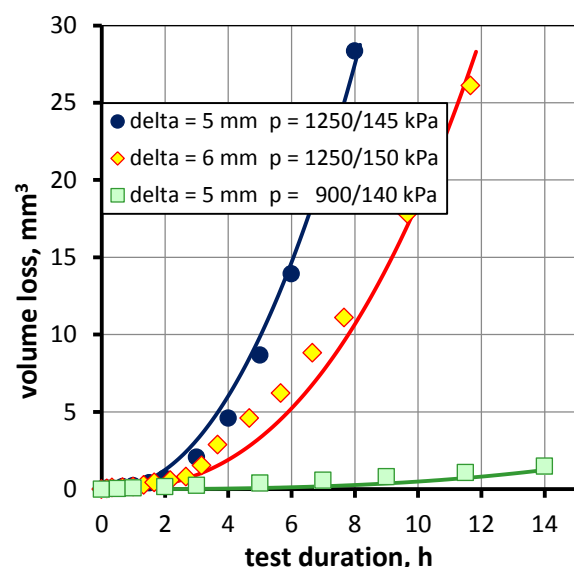


Fig. 4. Armco iron erosion curves depending on exposure time and test conditions

3.2. ANALYSIS OF THE RESULTS OF TESTS IN A CAVITATION TUNNEL (SITNIK'S FORMULA)

Based on the results of measurements of the distribution of cavitation load, the erosion curves of Armco iron were recalculated depending on the indicator of the supplied energy flow (Fig. 5).

As we can see, for Armco iron the erosion rate shows a weak dependence on the qualitative properties of the delivered energy flow. As a result, Armco iron can serve as a reference material for determining the integral value of the delivered energy flow indicator in other devices.

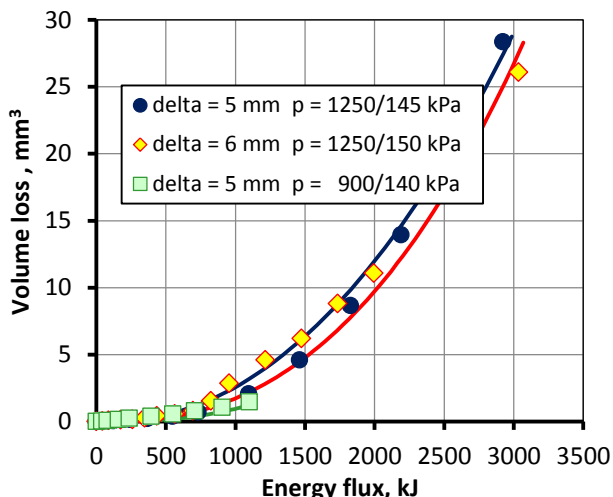


Fig. 5. Armco iron erosion curves depending on the delivered energy flow rate

For further discussion it is important to assume that the parameter ME represents the density of the energy flux supplied to the surface, or can be considered at least proportional to it. With this assumption, the performance of the material under monofractional loading is characterized by a set of numerical parameters \mathbf{R} (resistance vector), and the loss of volume after exposure of duration t can be described by some analytical formula $\Delta V = A U(\mathbf{R}, Y)$.

As a model function U , the logarithmic exponential function used earlier by L. Sitnik [18] as the most adequate was used. The selected function is expressed by the formula:

$$V = V_0 \left[\ln \left(\frac{E}{E_0} + 1 \right) \right]^\beta \quad (1)$$

or

$$MDE = MDE_0 \left[\ln \frac{Y}{Y_0} + 1 \right]^\beta, \quad (2)$$

where $MDE = V/A$ denotes the average depth of erosion over a surface area A ; $MDE_0 = V_0/A$ is the corresponding proportionality coefficient; $E = A \cdot ME \cdot t$ and $E_0 = A \cdot ME \cdot t_0$ are quantities proportional to the energy flux delivered to the surface A over a period of time t and t_0 , $Y = E/A$ and $Y_0 = E_0/A$, representing the densities of this flux, respectively:

$$V = V_0 \left[\ln \left(\frac{E}{E_0} + 1 \right) \right]^\beta = A \cdot MDE_0 \left[\ln \frac{Y}{Y_0} + 1 \right]^\beta. \quad (3)$$

Reverse function

$$Y = \theta(MDE) = Y_0 \left[\exp \left(\frac{MDE}{MDE_0} \right)^{1/\beta} - 1 \right] \quad (4)$$

or

$$Y = Y_0 \left[\exp(V/V_0)^{1/\beta} - 1 \right]. \quad (5)$$

3.3. CALCULATED DATA

The results of calculations using the L. Sitnik formula in the FRACTOR program are shown in Fig. 6 and Table 1.

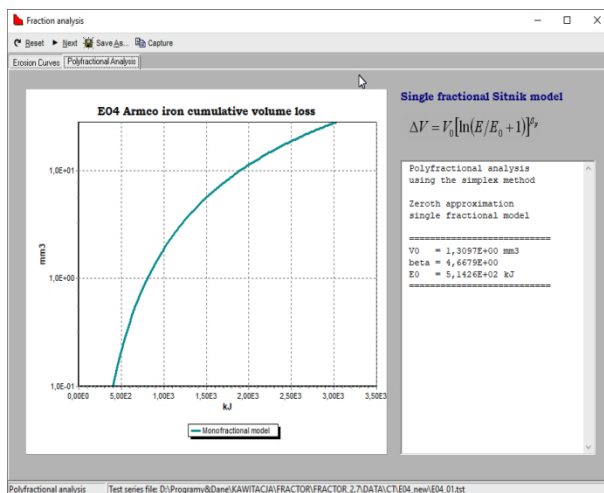


Fig. 6. Computer screen with FRACTOR program calculation results

Table 1

Constants of the erosion depth curve according to L. Sitnik

V_0	m^3	1.3079E-09
E_0	kJ	5.1426E+02
A	m^2	5.12E-04
MDE_0	m	2.55449E-06
β		4.6679
Y_0	kJ/m^2	1.0044E+06

3.4. ESTIMATION OF DISTRIBUTION OF CAVITATION LOAD ON THE SURFACE OF A SAMPLE FOR A ROTATING DISK INSTALLATION (SITNIK'S FORMULA)

The load distribution was determined on an Armco iron sample after 6 h of testing by the rotating disk method in the laboratory of the IPM PAN in Gdansk. The appearance and erosion profiles of the sample are shown in Fig. 7.

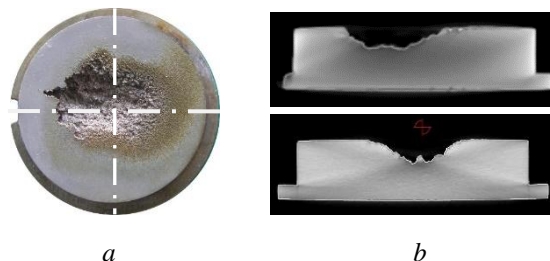


Fig. 7. Armco iron after 6 h of testing (a), and diametrical tomographic sections of the sample (b)

Erosion profiles were extracted from 3D X-ray tomograms of Armco-iron samples after testing on a rotating disk rig. The surface load distribution was then determined from these profiles using the previously calculated Sitnik erosion depth curve constants. Table 2

shows examples of the averaged local load calculation, and Fig. 8 shows the dependence of the load by the diameter of the Armco iron sample.

Table 2

Example of calculation of average local load of Armco iron (e.g. rotating disk)

MDE	mm	0.5	1	2
MDE	m	0.0005	0.001	0.002
t	min	360	360	360
t	s	21600	21600	21600
Y	kJ	8.17E+06	1.34E+07	2.38E+07
ME	kW/m ²	3.78E+02	6.21E+02	1.10E+03

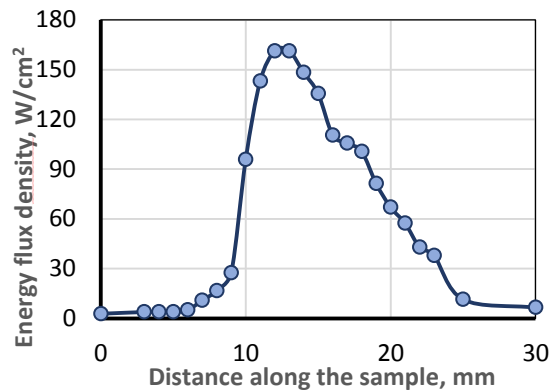


Fig. 8. Dependence of the cavitation load along the diameter of the armco iron sample

The obtained results were used to determine the dependence of the fraction of the removed protective TiN coating (applied by the Arc-PVD method at NSC KIPT) on titanium and stainless steel on time under various local loads during tests on a cavitation station with a rotating disk (IPM PAN). Simultaneous testing of several samples under the same conditions provides valuable information on their behavior under cavitation load. Fig. 9 shows images of Armco samples of iron, titanium and coatings on titanium and stainless steel. As we can see, there are significant differences in their erosion resistance.



Fig. 9. Samples after rotating disk testing. Top left right – Armco iron (6 h), Ti (0.5 h); bottom – TiN/SS, (0.5 h), TiN/Ti (0.5 h)

When testing protective coatings, the probability of their complete removal after a given period of time is of primary interest. The dynamics of TiN coating removal from titanium on a rotating disk station depending on the test time is shown in Figs. 10 and 11 also shows the erosion zones of uncoated titanium depending on the test time with the cavitation load curve superimposed on them. As we can see, there is a clear correlation between the magnitude of the local load and the test time.

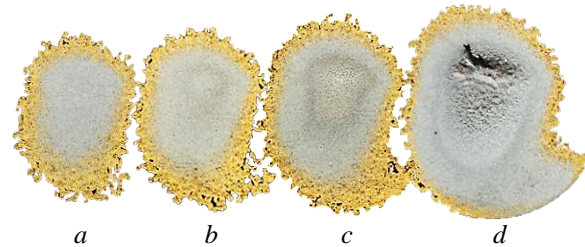


Fig. 10. View of removal of TiN coating on titanium under cavitation load on a rotating disk station from the test time: a – 15; b – 30; c – 60; d – 360 min

Summary of results for two batches of samples with TiN coating on titanium alloy and stainless steel are presented in Fig. 12. As can be seen from these dependencies, the erosion resistance of the TiN coating depends significantly on the substrate material.

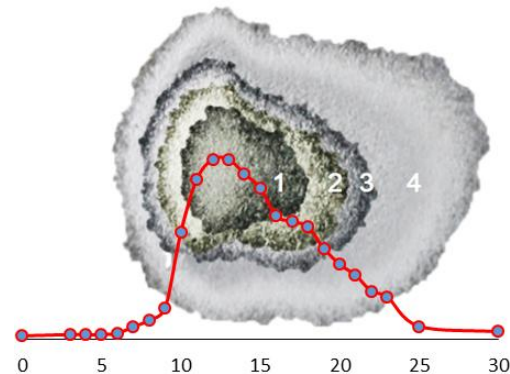


Fig. 11. Titanium alloy erosion zone depending on test time: 1 – 15; 2 – 30; 3 – 60; 4 – 360 min and the cavitation load curve (see Fig. 8)

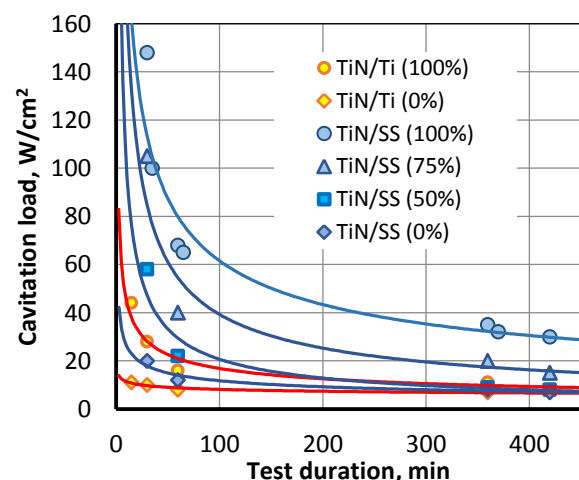


Fig. 12. Exposure duration to reach specified coating removal degree (%) of TiN coatings on the titanium alloy and X10CrNiTi 18-10 steel substrates vs cavitation load parameter

The progress of TiN/Ti and TiN/SS coating removal degree at sites featured by different load density is shown in Fig. 13,a.

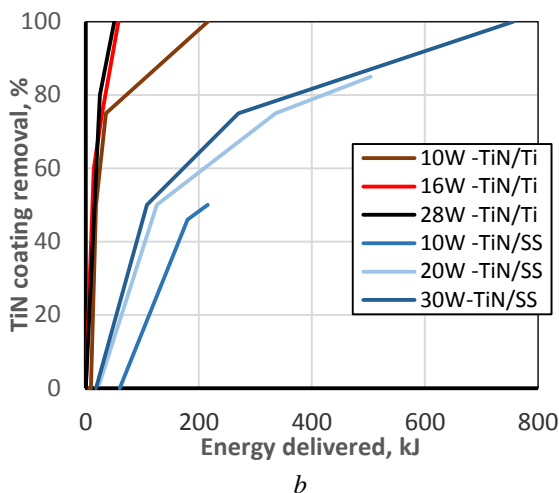
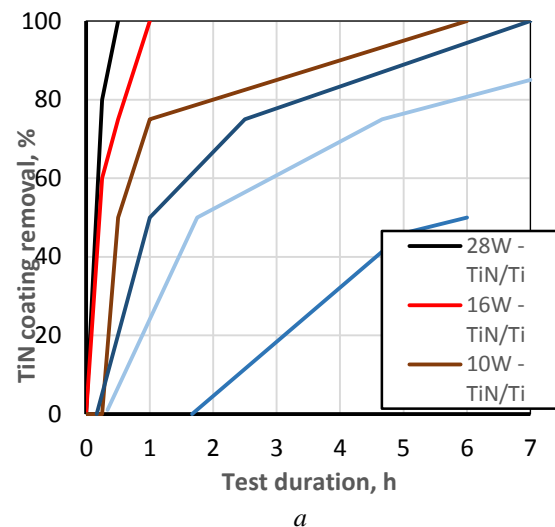


Fig. 13. The removed fraction of the TiN protective coating surface when tested under various local loads at the cavitation rotating disk station as plotted exposure duration (a) and delivered energy density parameter (b)

According to the monofractional approach, the plots vs the delivered energy density parameter, $E = ME t$, are expected to overlap which allows to use ME as the sole cavitation intensity characteristics. As it can be seen from Fig. 13,b, this expectation is generally fulfilled only under certain circumstances – e.g. sufficiently high load and/or coating removal degree below certain threshold. In case of coatings under consideration the threshold values are above 10 W/cm^2 and 50%, respectively. Extending the coating erosion prediction capability onto the whole coating removal curve requires consideration of some qualitative load features, like the local histograms of cavitation pulse amplitudes. A relevant methodology (polyfractional approach) is described in the second part of our contribution [19].

CONCLUSIONS

This paper presents a new methodology for assessing the cavitation load and durability of structural materials and protective coatings in a monofraction approach.

In view of the structural complexity of determining the cavitation load on a rotating disk facility, a new method for extracting erosion loads was proposed based on testing reference materials on a reference flow rig.

Armco iron was chosen as a reference material, in view of the weak dependence of its erosion rate on cavitation qualitative features. This allows it to be used as a standard for measuring the integral cavitation load flux.

Direct measurements of the cavitation load in a cavitation tunnel with a slot cavitator were performed using piezoelectric sensors installed flush with the impinged surface plane. The measurements in the cavitation erosion zone provided information on the spatial distribution of the cavitation load.

The main idea of the method is to determine the scalar parameter of the cavitation load ME from the erosion curves of the reference material Armco iron obtained as a result of erosion tests at strictly defined cavitation loads on a reference test rig. To determine the erosive cavitation load on another test rig, for example, on a rotating disk, the eroded surface profile of the Armco iron sample is analyzed and the local load value is extracted. The curve of the average depth of erosion (MDE) due to the load in a monofractional approach was described using an analytical function of the form $U = U(R, Y)$, where R is the cavitation resistance vector depending on the properties of the material; Y is the surface density of the supplied energy measured using the energy flux density coefficient ME . The curve – fitting technique is applied in order to derive the erosion parameters of Armco iron (R vector). The logarithmic formula of L. Sitnik (2) is used as an analytical function for modeling the curves of cumulative erosion in a single-fraction approach. L. Sitnik's model assumes that cavitation erosion is a stochastic process described using fatigue theory. By using the reversed formula (2) it is easy to establish the energy density parameter necessary to penetrate the sample at the depth following from the sample surface analysis procedures.

Using the example of TiN coating analysis on stainless steel and VT3-1 alloy, time dependencies and threshold characteristics of their resistance were determined depending on the delivered energy density parameter.

It can be expected that knowledge of the energy characteristics of cavitation loads (depending on exposure duration, pulse amplitude, and radial distribution) will allow to link them with the corresponding model of material reaction and will allow numerical prediction of the time evolution of damage.

However, for a more accurate interpretation of the results, it will be necessary to introduce a polyfractional analysis of the cavitation load.

ACKNOWLEDGEMENTS

This work was partially conducted within the framework of statutory scientific activities of the IMP PAN as well as research projects of the State Committee for Scientific Research and the Polish Ministry of Science and Higher Education. Further results from the joint work conducted by the authors within the cooperation agreement between the Polish Academy of

Sciences and the National Academy of Sciences of Ukraine. In 2023, this work was also partly funded by the European Fund for Displaced Scientists (EFDS), established by the European Federation of Academies of Sciences and Arts (ALLEA).

REFERENCES

1. Leonhard Euler. Théorie plus complete des machines qui sont mises en mouvement par la réaction de l'eau. 1756; <https://scholarlycommons.pacific.edu/euler-works/222>
2. L. Rayleigh. VIII. On the pressure developed in a liquid during the collapse of a spherical cavity // *Philosophical Magazine. Series 6*. 1917, v. 34(200), p. 94-98; <http://dx.doi.org/10.1080/14786440808635681>
3. G. Gao., S. Guo., D.A. Li. Review of Cavitation Erosion on Pumps and Valves in Nuclear Power Plants // *Materials*. 2024, v. 17, p. 1007; <https://doi.org/10.3390/ma17051007>
4. M.G. Haese, R. Skoda. Three-dimensional flow simulation and cavitation erosion modeling for the assessment of incubation time and erosion rate // *Wear*. 2023, v.524-525, p. 204747.
5. Tijsseling, A. Vardy, and D. Fan. Fluid-structure interaction and cavitation in a single-elbow pipe system // *Journal of Fluids and Structures*. 1996, v. 10, p. 395-420.
6. L. Geng, J. Chen, O. De La Torre, and X. Escaler. Numerical Simulation of Cavitation Erosion Aggressiveness Induced by Unsteady Cloud Cavitation // *Appl. Sci*. 2020, v. 10, p. 5184; doi:10.3390/app1015518
7. M.S. Plesset, A.T. Ellis. On the Mechanism of Cavitation Damage // *Trans. ASME*. 1955, v. 77(7), p. 1055-1064; <https://doi.org/10.1115/1.4014587>
8. A. Karimi, W.R. Leo. Phenomenological model for cavitation rate computation // *Materials Science and Engineering*. 1987, v. 95, p. 1-14.
9. J.P. Franc, F. Avellan, et al. La Cavitation. Mécanismes physiques et aspects industriels // *Presses Universitaires de Grenoble*. Grenoble, 1995, 581 p.
10. W. Bedkowski, G. Gasiak, C. Lachowicz, A. Lichtarowicz, T. Łagoda, E. Mach. Relations between cavitation erosion resistance of materials and their fatigue strength under random loading // *Wear*. 1999, v. 230, p. 201-209.
11. <https://www.neimagazine.com/news/framatom-e-contracted-for-reactor-vessel-mitigation-at-us-npps-9706125/>
12. Hitoshi Soyama. Cavitation Peening: A Review // *Metals*. 2020, v. 10, p. 270; doi:10.3390/met10020270
13. S. Hattori, R. Ishikura, Q. Zhang. Construction of database on cavitation erosion and analyses of carbon steel data // *Wear*. 2004, v. 257(9-10), p. 1022-1029.
14. S. Hattori, R. Ishikura. Revision of cavitation erosion database and analysis of stainless steel data // *Wear*. 2010, v. 268(1-2), p. 109-116.
15. S. Hattori, N. Mikami. Cavitation erosion resistance of stellite alloy weld overlays // *Wear*. 2009, v. 267(11), p. 1954-60.
16. A. Karimi, J.L. Martin. Cavitation erosion of materials // *International Metals Reviews*. 1986, v. 31(1), p. 1-26.
17. J. Steller. Erosive wear modelling by means of the fractional approach // *Wear*. 2021, v. 484-485, p. 15.
18. J. Steller. Koncepcja oceny odporności kawitacyjnej materiałów metodą frakcyjną // *Zeszyty Naukowe IMP PAN*, 561/1520/2015, IMP PAN Publishers, Gdansk, 2018, 328 p. (DSc thesis)
19. J. Steller, V. Safonov. New methodologies for assessing cavitation load and resistance of structural materials and protective coatings in nuclear power industry. Part II. Polyfractional approach // *Problems of Atomic Science and Technology*. 2024, N 4(152), p. 126-131.

Article received 25.07.2024

НОВІ МЕТОДИКИ ОЦІНКИ КАВІТАЦІЙНОГО НАВАНТАЖЕННЯ ТА ОПОРУ КОНСТРУКЦІЙНИХ МАТЕРІАЛІВ ТА ЗАХИСНИХ ПОКРИТТІВ У АТОМНІЙ ЕНЕРГЕТИЦІ. ЧАСТИНА I. МОНОФРАКЦІЙНИЙ ПІДХІД

Володимир Сафонов, Януш Стеллер, Ілля Клименко, Олександр Купрін

Представлено новий метод оцінки кавітаційного навантаження та довговічності конструкційних матеріалів та захисних покриттів у монофракційному підході. Для визначення кавітаційного навантаження на диску, що обертається, або іншому стенді запропонований новий метод вирахування ерозійних навантажень на основі випробувань еталонних матеріалів на еталонній кавітаційній установці. Прямі вимірювання кавітаційного навантаження у кавітаційній трубі з щільним збудником кавітації, які виконані за допомогою п'єзоелектричних датчиків, дозволили отримати інформацію про просторовий розподіл ударного навантаження. Як аналітична функція для моделювання кумулятивних кривих ерозії у монофракційному підході використана логарифмічна формула Л. Ситника, яка передбачає, що кавітаційна ерозія є стохастичним процесом, що описується за допомогою теорії втом. Як еталонний матеріал обрано армо-залізо, швидкість ерозії якого слабо залежить від кавітаційних навантажень різної інтенсивності. Значення локального навантаження витягувалося з профілю ерозії зразка армо-заліза після ерозійних випробувань. На прикладі аналізу покриттів TiN на нержавіючій сталі та титановому сплаві ВТ3-1 визначені часові залежності та порогові характеристики їх стійкості залежно від параметра щільності енергії, що підводиться.